A Novel CircRNA Circ_0001722 Regulates Proliferation and Invasion of Osteosarcoma Cells Through Targeting miR-204-5p/RUNX2 Axis

Shuai Gong[1], Yi Zhang[1], Lina Pang[1], Liye Wang[1], and Wei He[1]

[1]The First Affiliated Hospital of Zhengzhou University

April 18, 2023

Abstract

Osteosarcoma (OS) is the most prevalent primary fatal bone neoplasm in adolescents and children owing to limited therapeutic methods. Circular RNAs (circRNAs) are identified as vital regulators in a variety of cancers. However, the role of circRNAs in OS are still unclear. In our study, we evaluate the differentially expressed circRNAs in 3 paired OS and corresponding adjacent nontumor tissue samples by circRNA microarray assay, finding a novel circRNA, circ_001722, significantly upregulated in OS tissues and cells. Then we show that downregulation of circ_0001722 can suppress proliferation and invasion of human OS cells in vitro and in vivo. Computational algorithms predict miR-204-5p can bind with circ_0001722 and RUNX2 mRNA 3'UTR, which is verified by Dual-luciferase assay and RNA immunoprecipitation assay. Further functional experiments show that circ_-0001722 competitively binds to miR-873-3p and prevents it to decrease the level of RUNX2, which upregulates proliferation and invasion of human OS cells. In summary, our research firstly show that circ_001722 promotes the progression of OS via miR-204-5p/RUNX2 axis.

A Novel CircRNACirc_0001722 Regulates Proliferation andInvasion of Osteosarcoma Cells Through TargetingmiR-204-5p/RUNX2 Axis

Shuai Gong[1], Email address: shuaigong001@163.com;

Yi Zhang[2], Email address:feiyi030@126.com;

Lina Pang[1], Email address:18703899100@163.com;

Liye Wang[1] , Email address:wangly0505@126.com;

Wei He[1*], Email address: hewei726@zzu.edu.cn

[1]Department of Oncology, the First Affiliated Hospital of Zhengzhou University, Zhengzhou 450052, Henan Province, China

[2]Department of Orthopaedic Surgery, the First Affiliated Hospital of Zhengzhou University, Zhengzhou 450052, Henan Province, China

*Corresponding to Dr. and Prof. Wei He,

Department of Oncology, the First Affiliated Hospital of Zhengzhou University, No. 1 of Jianshe Road, Er-Qi district, Zhengzhou City 450052, Henan province, China;

Tel.: +86-371-66295953;

Fax.: +86-371-66295953;

Email address:*hewei726@zzu.edu.cn*

Abstract

Osteosarcoma (OS) is the most prevalent primary fatal bone neoplasm in adolescents and children owing to limited therapeutic methods. Circular RNAs (circRNAs) are identified as vital regulators in a variety of cancers. However, the role of circRNAs in OS are still unclear. In our study, we evaluate the differentially expressed circRNAs in 3 paired OS and corresponding adjacent nontumor tissue samples by circRNA microarray assay, finding a novel circRNA, circ_001722, significantly upregulated in OS tissues and cells. Then we show that downregulation of circ_0001722 can suppress proliferation and invasion of human OS cells*in vitro* and *in vivo* . Computational algorithms predict miR-204-5p can bind with circ_0001722 and RUNX2 mRNA 3'UTR, which is verified by Dual-luciferase assay and RNA immunoprecipitation assay. Further functional experiments show that circ_0001722 competitively binds to miR-204-5p and prevents it to decrease the level of RUNX2, which upregulates proliferation and invasion of human OS cells. In summary, our research firstly show that circ_001722 promotes the progression of OS via miR-204-5p/RUNX2 axis.

Keywords: Osteosarcoma; circRNA; miR-204-5p; Runx2; Proliferation; Invasion

Background

Osteosarcoma (OS) is the most prevalent primary malignant bone neoplasm causing substantial morbidity in adolescents and children [1]. It originates from mesenchymal cells and is characterized by rapid infiltrating growth, early lung metastasis and a high recurrence rate [2]. Studies have shown that the overall 5-year survival rate of patients with localized OS ranges between 65 ~ 75% and is only 20% for those with recurrent and metastatic tumors [3]. Despite advances in OS treatment approaches such as adjuvant chemotherapy and surgical resection, the survival rates have plateaued in the last 3 decades and are less than satisfactory [4]. Indeed, no specific diagnostic and prognostic biomarkers for OS have been found. Consequently, molecular studies aiming to identify promising therapeutic targets for OS are urgently needed. Circular RNAs (circRNAs) regulate various functions in eukaryotic cells [5]. Based on the order of splicing events and different intermediates, two mechanisms exist for the biogenesis of circRNAs: canonical spliceosome induced splicing and noncanonical lariat splicing [6, 7]. Accumulating studies have shown that circRNAs modulate diverse physiological and pathophysiological processes by sponging microRNAs (miRNAs), interacting with RNA binding proteins, and modulating epigenetic, transcriptional, or translational alterations in target genes as well [8–11]. Abnormal circRNA expression has been found to correlate with the pathogenesis of various cancers and to exert essential regulatory effects on gene expression, cell invasion, cell cycle progression, migration, apoptosis, and proliferation [12–14]. Moreover, circRNAs are thought to possess high diagnostic and therapeutic potential given their structural stability, evolutionary conservation, abundance and organ specificity [15, 16]. However, to date, the roles of circRNAs in OS are not clearly known.

This study evaluated the expression profiles of circRNAs in OS tissues using high-throughput sequencing. We found a novel circRNA, designated circ_001722, significantly upregulated in OS tissues and cells. Our experimental results indicated that circ_001722 exerted pro-oncogenic effects on OS proliferation and invasion through circ_001722/miR-204-5p/RUNX2 Axis. This preliminary study revealed that circ_001722 is a potential therapeutic target for OS.

Materials and Methods

Patients and OS samples

A series of 20 surgically resected fresh human OS and corresponding adjacent nontumor tissue samples were collected at the First Affiliated Hospital of Zhengzhou University (Zhengzhou, China) and snap-frozen in liquid nitrogen from July 2018 to January 2019. Among them, 3 pairs were used for circRNA microarray analysis. No patients had received any preoperative treatment. Clinical data of patients included in this study are detailed in Supplementary Table 1. Samples used in this study were approved by the Committees for Ethical Review of the First Affiliated Hospital of Zhengzhou University.

CircRNA microarray analysis

Three pairs of human OS and corresponding adjacent nontumor tissue samples were used for the circRNA microarray assay to determine differentially expressed circRNAs. The microarray hybridization was performed based on the manufacturer's standard protocols (Agilent Technologies, USA), which included purifying the RNA, transcribing it into fluorescent cRNA, and then hybridizing it onto the Human circRNA Arrays (Agilent Technologies, USA). Finally, the hybridized slides were washed, fixed and scanned to images by an Agilent Scanner G2505C. The data collection was performed using Agilent Feature Extraction software (version 11.0.1.1). The raw data were quantile normalized, and further data analysis was performed with the R software package, GeneSpring GX (Agilent Technologies, USA) and gene expression dynamics inspector (GEDI). The statistical significance of differentially regulated circRNAs between OS tissue (T) and adjacent nontumor tissue (N) was identified through p-values and fold changes. Significantly differentially expressed transcripts were retained by screening for a fold change [?] 2.0 and $P < 0.05$. Hierarchical clustering was performed to generate an overview of the characteristics of expression profiles based on the values of all expressed transcripts and significant differentially expressed transcripts.

Circular structure confirmation

The circular structure of circ_0001722 was confirmed by RNase R treatment and Sanger sequencing by divergent primer PCR. For RNase R treatment, 3 μg total RNA extracted from OS tissues and cell lines were incubated with 20 U RNAse R (Epicentre Biotechnologies, USA) in a 10 μl volume at 37 °C for 45 min, followed by 70 °C for 10 min to deactivate the RNase R. The treated RNAs were used for RT-PCR. For Sanger sequencing, PCR products amplified by divergent primers of circ_0001722 were inserted into the T vector and sequenced by Tsingke Biotechnology (Beijing) Co., Ltd. The result was crosschecked with the back-splicing junction sites of circ_0001722 supplied by circBASE [17].

Cell culture, transfection, and lentiviral infection

Two human OS cell lines (MG63 and U2OS), a normal human fetal osteoblastic cell line (hFOB1.19) and a human embryonic kidney cell line (HEK293T) used in this study were purchased from Chinese National Collection of Authenticated Cell Cultures. MG63 cells were cultured in DMEM medium (Hyclone, USA) supplemented with 10% fetal bovine serum (HyClone, USA) and 1% penicillin/streptomycin (Invitrogen, USA) at 37 °C under 5% CO_2 and saturated moisture. U2OS cells were cultured in McCoy's 5a medium (Hyclone, USA) supplemented with 10% fetal bovine serum (HyClone, USA) and 1% penicillin/streptomycin (Invitrogen, USA) at 37 °C under 5% CO_2 and saturated moisture. hFOB1.19 cells were cultured in DMEM/F12 (1:1) medium (Hyclone, USA) supplemented with 10% fetal bovine serum (HyClone, USA) and 1% penicillin/streptomycin (Invitrogen, USA) at 37 °C under 5% CO_2 and saturated moisture. HEK293T cells were cultured in DMEM/high glucose medium (Hyclone, USA) supplemented with 10% fetal bovine serum (HyClone, USA) and 1% penicillin/streptomycin (Invitrogen, USA) at 37 °C under 5% CO_2 and saturated moisture. The authenticity of cell lines was verified by DNA fingerprinting before use. MiR-204-5p and its negative control (miR-NC), RUNX2 eukaryotic expression recombinant pIRESpuro2-RUNX2 were transfected transiently into OS cells using Lipofectamine 3000 (Invitrogen, USA) according to the manufacturer's instructions. To prepare sh-circ_0001722 lentiviral particles, the lentiviral vector harboring sh-circ_0001722 full hairpin sequence and packaging vectors were transfected into HEK293T cells using iMFectin Poly DNA Transfection Reagent (GenDEPOT, USA) following the manufacturer's suggested protocols. The transfection medium was changed at 8 h after transfection and then cells were cultured for 36 h. The lentiviral particles were harvested by filtration using a 0.45 μm sodium acetate syringe filter and then combined with 8 μg/ml of polybrane (Millipore, USA) and infected overnight into 60% confluent OS cells. The cell culture medium was replaced with fresh complete growth medium and after 24 h, cells were selected with 2 μg/ml of puromycine for an additional 24 h. The selected cells were used for experiments. MiR-204-5p mimic and its negative control (miR-NC), pIRESpuro2-RUNX2 vectors, lentiviral vectors harboring sh-circ_0001722 full hairpin sequence and mock sequence, were purchased from Shanghai GenePharma Co., Ltd.

RNA extraction and qRT-PCR analysis

Total RNA derived from human OS tissues and cells was isolated using TRIzol reagent (TAKARA, CHN) according to the manufacturer's instructions. RNA was reverse transcribed into cDNA using a Primer-Script one step RT-PCR kit (TAKARA, CHN). Quantitative real-time PCR experiments were performed using a SYBR Premix Dimmer Eraser kit (TAKARA, CHN) on an ABI 7500 Real-Time PCR System (Applied Biosystems, USA). The fold change in relative expression level was calculated using the 2^{-Ct} method. Relative circ_0001722 expression was normalized to GAPDH expression, and miR-204-5p expression was normalized to U6 small nuclear RNA (U6 snRNA). The primer sequences used in our study are purchased from Tsingke Biotechnology (Beijing) Co., Ltd and shown in Supplementary Table 2.

Cell proliferation assay

The proliferation of human OS cells was evaluated by the CellTiter 96 AQueous One Solution cell proliferation assay. human OS cells were plated in 96-well culture plates (3×10^3 per well). After 24 h of incubation, the cells were transfected with 30 pmol of target gene (sh-circ_0001722 or miR-204-5p or negative control) for 24, 48, 72, and 96 h. Then 20 μl Cell Titer 96 Aqueous One Solution (Promega, USA) were added and cells incubated for another 1 h. Absorbance was read at 492 nm.

Matrigel invasion assay

The invasion abilities of OS cells were evaluated using Transwell invasion chambers precoated with 50 μl of 2 mg/ml Matrigel (BD Biosciences, USA). In brief, 5×10^4 transfected cells suspended in 200 μl of serum-free DMEM were seeded into the upper chambers. A 600 μl volume of DMEM supplemented with 10% FBS was used as the attractant and was added into the lower chambers. After culture for 24 h, cells adhering to the lower surface of the membrane were fixed with paraformaldehyde (4%) and stained using crystal violet (0.1%), whereas cells on the upper surface of the membrane were removed by wiping with cotton swabs. At least three random fields of view containing cells that had migrated or invaded to the lower surface were imaged under an inverted light microscope.

Dual-luciferase assay

HEK293T cells were spread to 96 well plates at the concentration of 1×10^4 cells per well. After 24 hours, HEK293T cells were co-transfected with dual-luciferase reporter vector (pmirGLO-Wt-circ or pmirGLO-Mt-circ, pmirGLO-Wt-3'UTR or pmirGLO-Mt-3'UTR) and miR-204-5p mimics or negative control (miR-NC) using the Lipo-fectomine 3000 transfection reagent (Invitrogen, USA), respectively. After 48h of incubation, firefly and Renilla luciferase activities were measured using a dual-luciferase reporter assay system (Promega, USA) according to the manufacturer's instructions.

RNA immunoprecipitation (RIP) assay

The RIP assay was performed using a Magna RIP RNA Binding Protein Immunoprecipitation Kit (Bersinbio, China) according to the manufacturer's protocol. 2×10^7 MG63 or U2OS cells were lysed in complete RIP lysis buffer and the cell lysates were divided into two equal parts and incubated with either 5 μg human anti-Argonaute2 (AGO2) antibody (Millipore, USA) with rotation at 4°C overnight. Magnetic beads were added to the cell lysates and incubation was continued at 4°C for 1h. The samples were then incubated with Proteinase K at 55°C for 1h. The enriched RNA was obtained using RNA Extraction Reagent (Solarbio, CHN). The purified RNA was used to detect the expression levels of the genes of interest by qRT-PCR.

Western blot analysis

Protein concentrations of cell lysates were determined using a protein assay kit (Bio-Rad Laboratories, USA). Total proteins (20 μg) were separated by SDS-PAGE and transferred onto a polyvinylidene difluoride membrane (Millipore, USA). After blocking in 5% non-fat milk, the membranes were probed with primary antibodies (RUNX2: sc-101145, GAPDH: sc-47724, Santa Cruz Biotechnology, USA) overnight at 4 °C, then washed 3 times with TBS-Tween 20 followed by incubation at room temperature 1 h with a horseradish peroxidase (HRP)-conjugated secondary antibody. The protein bands were visualized with an Immobilon Western Chemiluminescent HRP Substrate (Millipore, USA).

Xenograft nude mouse model

Six-week-old male BALB/C nude mice (Vital River Laboratory Animal Technology, Beijing, CHN) were maintained under specific pathogen-free conditions with a 12h light/dark cycle. All animal experiments were performed in accordance with the guide lines for the Care and Use of Laboratory Animals of Zhengzhou University. MG63 cells stably transfected with sh-circ_0001722 lentivirus or control lentivirus were subcutaneously injected into the right upper back of the nude mice (5×10^6 cells per mouse). Four weeks later, the mice were sacrificed and tumor tissues were collected for examination of the parameters of interest.

Immunohistochemistry staining

Immunohistochemical analysis for Ki67 was performed on 4-μm sections. The Envision Plus detection system (Dako, USA) was used for the detection of immunostaining. Tissue sections were pretreated with 10 mM sodium citrate buffer for antigen unmasking (pH 6.0) after deparaffinized in xylene. Endogenous peroxidase activity was blocked by incubation with 0.03% hydrogen peroxide in methanol for 15 min. Then sections were incubated with Ki67 primary antibody (MA5-14520, Thermo Scientific, USA) at 4°C overnight after blocked in normal serum for 30min. Next, Sections were incubated with secondary antibody at room temperature for 60 min before staining for 5 min with 3'3-diaminobenzidine tetrahydrochloride, counterstained by hematoxylin, and observed by microscope (200×).

Statistical analysis

Data for continuous variables are presented as means ± standard deviations. All analyses were performed using SPSS 21.0 software (IBM, USA). All experiments were performed with three technical replicates, and at least three biological replicates were performed. Differences between groups were analyzed using unpaired Student's t-test or one-way analysis of variance (ANOVA) with Tukey's test. A P value of < 0.05 was considered to be statistically significant.

Results

The results ofcircRNA identification and annotation

The reads were aligned to the reference genome using bwa mem software. The read distribution of OS and corresponding adjacent nontumor tissues on the chromosomes were shown in Supplementary Figure 1a and 1b, separately. After bwa mem alignment, sam files were subjected to CIRI2 processing twice. Firstly, the junction reads were detected by paired chiastic clipping (PCC) signals. Basing on paired-end mapping (PEM) and GT-AG sequence feature, the reads were preliminary filtered to obtain candidate circRNAs. Secondly, the junction reads were detected again to filter out the false-positive candidate circRNAs (Supplementary Figure 1c). Totally, 6646 circRNAs were identified in OS and nontumor tissues, and in each type of samples, with 1-3 circRNAs on most genes. Among these 6646 circRNAs, 6014 circRNAs were distributed on exon region, 459 circRNAs were distributed on intron region, and the rest 173 circRNAs were distributed on intergenic region. Moreover, 4275 circRNAs have been annotated before, and the remaining 2371 were newly annotated. The lengths of 6646 circRNAs were mainly distributed in the range of 150-1000 bp (Supplementary Figure 1d).

Differentially expressed circRNAs and circRNA/miRNA/mRNA regulatory network

Additionally, we have also identified the differentially expressed circRNAs between OS and corresponding adjacent nontumor tissue samples. Compared with nontumor samples, there were totally 1088 significantly differentially expressed circRNAs in OS samples, including 1052 upregulated circRNAs and 36 downregulated circRNAs (Figure 1a). The expression levels of differentially expressed circRNAs were significantly different (Figure 1b).

Furthermore, we have estimated the circRNA/miRNA interactions using miRanda and TargetScan. After the cross analysis of predicted results of two software, there were 36 differentially expressed circRNAs and their corresponding miRNAs in regulatory network (Supplementary Figure 2a). Among them, circ_0001722 with small expression standard deviations in three OS samples and three nontumor samples (standard deviation

values were 3.1 and 0.7, respectively) was selected for subsequent analysis. Regarding circ_0001722, there were 11 overlapped regulatory pairs between miRanda and TargetScan (Supplementary Figure 2b), including miR-365b-5p, miR-3122, miR-211-5p, miR-208b-5p, miR-3913-5p, miR-204-5p, miR-365a-5p, miR-5006-3p, miR-208a-5p, miR-3137 and miR-6875-3p. Then, the target genes of these 11 miRNAs were also estimated utilizing miRTarBase database. We found that miR-204-5p and its corresponding 76 target genes, comprising RUNX2, were supported by most experimental validation (469 experimental results). The circRNA/miRNA/mRNA regulatory network, based on circ_0001722, 11 miRNAs, and target mRNAs, was shown in Figure 1c.

Expression of circ_0001722 is significantly upregulated inOS tissues and cell lines

Firstly, we determined whether circ_0001722 is a closed circular RNA that is resistant to RNase R digestion. We investigated its expression level in OS tissues and cell lines. Our result showed that RNase R digestion could decrease the RNA level of linear GAPDH, but could not affect the level of circ_0001722 significantly (Figure 1d), indicating that circ_0001722 was resistant to RNase R digestion. To confirm circ_0001722 is a closed circRNA, we ran PCR amplification of circ_0001722 with specific divergent primers. PCR products amplified by divergent primers were detected by Sanger sequencing to confirm the circular structure of circ_0001722. Our data showed that the back splicing junction sites of circ_0001722 were consistent with the sequence from circBase (Figure 1e). Then, we measured the expression level of circ_0001722 in a series of 20 surgically removed fresh OS tissues and their corresponding adjacent nontumor tissues by qRT-PCR. Comparing with nontumor tissues, the expression level of circ_0001722 in OS tissues was significantly upregulated (P <0.01; Figure 1f). Similarly, the expression of circ_0001722 in OS cell lines (MG63 and U2OS) was significantly higher than in normal human fetal osteoblastic cell line (hFOB 1.19) (P <0.01; Figure 1g).

Downregulation ofcirc_0001722 suppresses cell proliferation of human OS cells *in vitro* and *in vivo*.

We noticed that the expression of circ_0001722 was higher in MG63 cells and U2OS cells. Based on the observation, exogenous shRNA (sh-circ_0001722) was used to knock down circ_0001722 expression in two OS cell lines (Figure 2a). Based on the high silencing efficiency, we carried out cell proliferation assay and matrigel invasion assay. The results showed that the viability level of MG63 cells and U2OS cells transfected with sh-circ_0001722 was lower than that of the cells transfected with sh-Mock (Figure 2b). Consistently, sh-circ_0001722 significantly decreased the number of OS cells invaded through the matrigel. Quantitative analysis of cell numbers revealed that, in the negative control (sh-Mock) and blank control groups, the number of cells invaded through the matrigel was almost 5 times higher than sh-circ_0001722 group (figure 2c). The above experiments verified to some extent that silencing circ_0001722 can inhibit the proliferation and invasion of OS cells *in vitro* . To investigate whether circ_0001722 regulates the tumorigenesis of OS *in vivo* , we established OS xenograft mouse models. MG63 cells transfected with sh-circ_0001722 or sh-Mock were inoculated subcutaneously in the right flank of athymic nude mice (5×10^6 cells per mouse, 5 mice per group). After 4 weeks, all experimental mice were euthanized and tumor tissues were collected (Figure 2d). Comparing with sh-Mock group, smaller tumor volume and lower tumor weight were observed in sh-circ_0001722 group. The same conclusion was reached with the*in vitro* experimental results. Downregulation of circ_0001722 can suppress tumorigenesis of OS cells *in vivo* . In addition, compare with the control group, knocking down of circ_0001722 led to the decrease of Ki67 expression, which implied the cell proliferation of sh-circ_0001722 group is slower than sh-Mock group. Taken altogether, downregulation of circ_0001722 can restrain the growth of OS cells*in vitro* and *in vivo* .

Circ_0001722 acts as a sponge for miR-204-5p.

The sequences of circRNAs are highly conservative, and circRNAs can function as miRNA sponge to regulate gene expression. Through bioinformatical analysis, we discovered that complementary pairing sites (80-89 nt) on circ_0001722 that could bind to miR-204-5p (Figure 3a). To validate binding capability of the miR-204-5p to circ_0001722, we constructed the circ_0001722 luciferase reporter system. In the dual-luciferase reporter assay, comparing with miR-NC, miR-204-5p mimics could significantly suppressed the luciferase activity of pmirGLO-Wt-circ in HEK293T cells, while the luciferase activity of pmirGLO-Mt-circ could not

be suppressed (Figure 3b). We next performed Ago2 immunoprecipitation to determine whether circ_0001722 served as a platform for Ago2 and miR-204-5p. As shown in Figure 3c, circ_0001722 and miR-204-5p were abundantly enriched more in Ago2 protein than in IgG, suggesting that expression of miR-204-5p could be affected by circ_0001722. Moreover, the expression of miR-204-5p was elevated in circ_0001722 silenced MG63 and U2OS cells (Figure 3d). Furthermore, the results of Pearson's correlation analysis showed the circ_0001722 level was inversely to correlate with miR-204-5p level in 20 human OS tissues (Figure 3e), which providing evidence of the potential correlation between circ_0001722 and miR-204-5p. Given all of these data, circ_0001722 not only targeted miR-204-5p but also acted as a sponge for miR-204-5p in OS cells.

Sh-circ_0001722 inhibits the proliferation and invasion of human OS cells by upregulating miR-204-5p.

In order to further investigate whether circ_0001722 plays a promotion role in OS cells through binding with miR-204-5p, we conducted the following experiments. We transfected MG63 and U2OS cells with miR-204-5p, making miR-204-5p expression increased remarkably, which also could be observed after sh-circ_0001722 transfection as well (Figure 4a). The cell proliferation assays showed that both upregulation of miR-204-5p and downregulation of circ_0001722 could suppress OS cell proliferation ability *in vitro* (Figure 4b). Transwell assay showed that cell invasion was remarkably restrained after sh-circ_0001722 or miR-204-5p transfection (Figure 4c). These findings demonstrated that miR-204-5p contributed to proliferation and invasion of OS cells, and sh-circ_0001722 reduced tumorigenesis in OS cells by directly binding and upregulating miR-204-5p.

Sh-circ_0001722 mediates OS cells suppression through the miR-204-5p /RUNX2 axis.

Computational algorithms predicted that miR-204-5p could specifically bind to complementary sequence (268-274 nt) of RUNX2 3'UTR (Figure 5a). We carried out the 3'UTR luciferase reporter assay to verify whether miR-204-5p can bind to RUNX2 3'UTR and inhibit its expression. The result showed that miR-204-5p could significantly reduce the luciferase activity of pmirGLO-Wt-3'UTR clone, but could not affect the luciferase activity of pmirGLO-Mt-3'UTR clone (Figure 5b), indicating that miR-204-5p can directly target the 3'UTR of RUNX2 mRNA, leading to the inhibition of its translation. In addition, Western blotting analysis showed that, both miR-204-5p and sh-circ_0001722 could induce a significantly reduction of endogenous RUNX2 expression in OS cells (Figure 5c). Moreover, rescue assays showed that the cell proliferation ability inhibited by sh-circ_0001722 could be rescued by exogenous RUNX2 (Figure 5d). The inhibitory effect of sh-circ_0001722 on cell invasion could also be rescued by exogenous RUNX2 as well (Figure 5e). Our results verified that miR-204-5p contributed to proliferation and invasion of OS cells through targeting RUNX2 mRNA, and sh-circ_0001722 reduced tumorigenesis of OS cells by directly binding and upregulating miR-204-5p/RUNX2 axis.

Discussion

OS is the most prevalent malignant bone tumor. It is highly metastatic, resulting in a very poor survival rate [2]. Approximately 80% of OS patients exhibit subclinical pulmonary micro metastases at the time of diagnosis [18]. The lack of accurate biomarkers has further hindered efforts to improve the clinical outcome of OS. Recently, the dysregulation of ncRNAs in OS has generated significant interest from scientific communities. Being different from the other miRNAs or lncRNAs, circRNAs have emerged as more reliable and promising tumor biomarkers owing to their exceptionally stable structure. Advanced genome sequencing techniques have validated the roles of circRNAs in multiple cancers, including hepatocellular carcinoma [19], gastric cancer [20], colorectal cancer [21] and lung squamous cell carcinoma [22]. However, to date, the expression profiles and roles of circRNAs in OS are not well understood.

Our study provides the first evidence that circ_001722 contributes to the malignant progression of OS. CircRNAs are widely accepted to be an unorthodox RNA species generated by alternative splicing of pre-mRNAs [23]. There are three main classes of circRNAs: exonic circRNAs, exon-intron circRNAs and intronic circRNAs [24]. Herein, we revealed upregulated expression of circ_001722 in OS tissues and cells using high-throughput sequencing and qRT-PCR. Functional analyses further validated the role of circ_001722 in promoting the proliferation and metastasis of OS cells both *in vivo* and *in vitro* .

The subcellular distribution of RNAs is intimately tied to their biological functions [25]. Accumulating evidence shows that cytoplasmic circRNAs sponge miRNAs, which represses the translation or induces the degradation of the target mRNAs. Herein, through bioinformatical analysis, we discovered that complementary pairing sites on (82-89 nt) circ_0001722 that can bind to miR-204-5p. Despite this new finding, the involvement of miR-204-5p in the pathogenesis of multiple tumors is not a new phenomenon. Reports on the interactions between miR-204-5p and circRNAs in cancer are scarce. Herein, we found that miR-204-5p expression was inversely correlated with circ_001722. Functional rescue experiments further revealed that the miR-204-5p inhibitor substantially reversed the suppressive effects of circ_001722 depletion on proliferation and metastasis of OS cells, whereas miR-204-5p could abolish the promotive effects of circ_001722 overexpression.

Moreover, we found that RUNX2 is a downstream target of miR-204-5p in OS cells. Functional experiments revealed that circ_001722 upregulated RUNX2 expression by sponging miR-204-5p. But, RUNX2 triggered which pathway activation to accelerate OS progression via mechanisms including suppression of apoptosis and promotion of cell proliferation, migration and invasion, still need to explore. Evidence indicates that RUNX2 is implicated in diverse biological processes, including bone development, tumor invasion and metastasis [26, 27]. Initial findings indicate the carcinogenesis mediated by the circ_001722/miR-204-5p/RUNX2 axis in OS.

Conclusions

In summary, our research firstly showed that circ_001722 promotes the progression and metastasis of OS via the circ_001722/miR-204-5p/RUNX2 axis. Our findings elucidate a novel regulatory network that may offer new insight into the identification of potential biomarkers or therapeutic targets for OS.

Declarations

Ethics approval and consent to participate

All aspects of this study were approved by Institutional Research Ethics Committee of the First Affiliated Hospital of Zhengzhou University. Written informed consents were obtained from all participants

Consent for publication

Not applicable.

Availability of data and material

All data are fully available without restrictions.

Competing interests

The authors declare no competing interests.

Funding

This work was supported by National Natural Science Foundation of China (82102715), the Foundation of Henan Educational Committee (21A320030) and the Henan Provincial Science and Technology Research Project (212102310126).

Authors' contributions

WH contributed to the conception of the study; YZ collected clinical cases; SG and LNP performed the experiment; SG contributed to analysis and manuscript preparation; SG and LYW performed the data analyses; WH and SG wrote the manuscript; WH made contributions to quality control of the study and to critical revision of the manuscript; all authors have read and approved the final manuscript.

Acknowledgements

Not applicable.

Data Availability

All data are fully available without restrictions.

Acknowledgements

This work was supported by National Natural Science Foundation of China (82102715), the Foundation of Henan Educational Committee (21A320030) and the Henan Provincial Science and Technology Research Project (212102310126).

Contributions

HW contributed to the conception of the study; ZY collected clinical cases; GS and PLN performed the experiment; GS contributed to analysis and manuscript preparation; GS and WLY performed the data analyses; HW and GS wrote the manuscript; HW made contributions to quality control of the study and to critical revision of the manuscript; all authors have read and approved the final manuscript.

References

[1] Ritter J, Bielack SS. Osteosarcoma. Ann Oncol. 2010;21(Suppl 7):i320–5.

[2] Ottaviani G, Jaffe N. The epidemiology of osteosarcoma. Cancer Treat Res. 2009;152:3–13. https://doi.org/10.1007/978-1-4419-0284-9_1.

[3] Miwa S, Shirai T, Yamamoto N, Hayashi K, Takeuchi A, Igarashi K, et al. Current and emerging targets in immunotherapy for osteosarcoma. J Oncol. 2019;2019:7035045.

[4] Bielack SS, Kempf-Bielack B, Delling G, Exner GU, Flege S, Helmke K, et al. Prognostic factors in high-grade osteosarcoma of the extremities or trunk: an analysis of 1,702 patients treated on neoadjuvant cooperative osteosarcoma study group protocols. J Clin Oncol. 2002;20(3):776–90. https://doi.org/10.1200/JCO.2002.20.3.776.

[5] Meng S, Zhou H, Feng Z, Xu Z, Tang Y, Li P, et al. CircRNA: functions and properties of a novel potential biomarker for cancer. Mol Cancer. 2017;16(1): 94. https://doi.org/10.1186/s12943-017-0663-2.

[6] Chen LL, Yang L. Regulation of circRNA biogenesis. RNA Biol. 2015;12(4): 381–8. https://doi.org/10.1080/15476286.2015.1020271.

[7] Zhou WY, Cai ZR, Liu J, Wang DS, Ju HQ, Xu RH. Circular RNA: metabolism, functions and interactions with proteins. Mol Cancer. 2020;19(1):172. https:// doi.org/10.1186/s12943-020-01286-3.

[8] Ashwal-Fluss R, Meyer M, Pamudurti NR, Ivanov A, Bartok O, Hanan M, et al. Kadener S: circRNA biogenesis competes with pre-mRNA splicing. Mol Cell. 2014;56(1):55–66. https://doi.org/10.1016/j.molcel.2014.08.019.

[9] Du WW, Yang W, Liu E, Yang Z, Dhaliwal P, Yang BB. Foxo3 circular RNA retards cell cycle progression via forming ternary complexes with p21 and CDK2. Nucleic Acids Res. 2016;44(6):2846–58. https://doi.org/10.1093/nar/gkw027.

[10] Su M, Xiao Y, Ma J, Tang Y, Tian B, Zhang Y, et al. Circular RNAs in Cancer: emerging functions in hallmarks, stemness, resistance and roles as potential biomarkers. Mol Cancer. 2019;18(1):90.*https://doi.org/10.1186/s12943-019-1*002-6.

[11] Li Z, Huang C, Bao C, Chen L, Lin M, Wang X, et al. Exon-intron circular RNAs regulate transcription in the nucleus. Nat Struct Mol Biol. 2015; 22(3): 256–64.*https://doi.org/10.1038/nsmb.2959*.

[12] Wang D, Yang S, Wang H, Wang J, Zhang Q, Zhou S, et al. The progress of circular RNAs in various tumors. Am J Transl Res. 2018;10(6):1571–82.

[13] Li Z, Yanfang W, Li J, Jiang P, Peng T, Chen K, et al. Tumor-released exosomal circular RNA PDE8A promotes invasive growth via the miR-338/MACC1/MET pathway in pancreatic cancer. Cancer Lett. 2018;432:237–50. https://doi.org/10.1016/j.canlet.2018.04.035.

[14] Zhao ZJ, Shen J. Circular RNA participates in the carcinogenesis and the malignant behavior of cancer. RNA Biol. 2017;14(5):514–21. *https://doi.org/1*0.1080/15476286.2015.1122162.

[15] Rybak-Wolf A, Stottmeister C, Glažar P, Jens M, Pino N, Giusti S, et al. Circular RNAs in the mammalian brain are highly abundant, conserved, and dynamically expressed. Mol Cell. 2015;58(5):870–85.*https://doi.org/10.1016/j.* molcel.2015.03.027.

[16] Cui X, Wang J, Guo Z, Li M, Li M, Liu S, et al. Emerging function and potential diagnostic value of circular RNAs in cancer. Mol Cancer. 2018;17(1): 123.*https://doi.org/10.1186/s12943-018-0877-y.*

[17] Chen X, Zhou Y, Liu S, Zhang D, Yang X, Zhou Q, et al. LncRNA TP73-AS1 predicts poor prognosis and functions AS oncogenic lncRNA in osteosarcoma. J Cell Biochem. 2018.

[18] Jaffe N. Osteosarcoma: review of the past, impact on the future. The American experience. Cancer Treat Res. 2009;152:239–62. https://doi.org/10.1007/978-1-4419-0284-9_12.

[19] Xu J, Ji L, Liang Y, Wan Z, Zheng W, Song X, et al. CircRNA-SORE mediates sorafenib resistance in hepatocellular carcinoma by stabilizing YBX1. Signal Transduct Target Ther. 2020;5(1):298. https://doi.org/10.1038/s41392-020-00375-5.

[20] Niu Q, Dong Z, Liang M, Luo Y, Lin H, Lin M, et al. Circular RNA hsa_circ_0001829 promotes gastric cancer progression through miR-155-5p/SMAD2 axis. J Exp Clin Cancer Res. 2020;39(1):280. https://doi.org/10.1186/s13046-020-01790-w.

[21] Wu M, Kong C, Cai M, Huang W, Chen Y, Wang B, et al. Hsa_circRNA_002144 promotes growth and metastasis of colorectal cancer through regulating miR-615-5p/LARP1/mTOR pathway. Carcinogenesis. 2020.

[22] Harrison EB, Porrello A, Bowman BM, Belanger AR, Yacovone G, Azam SH, et al. A circle RNA regulatory Axis promotes lung squamous metastasis via CDR1-mediated regulation of Golgi trafficking. Cancer Res. 2020;80(22):4972–85. https://doi.org/10.1158/0008-5472.CAN-20-1162.

[23] Jia GY, Wang DL, Xue MZ, Liu YW, Pei YC, Yang YQ, et al. CircRNAFisher: a systematic computational approach for de novo circular RNA identification. Acta Pharmacol Sin. 2019;40(1):55–63. https://doi.org/10.1038/s41401-018-0063-1.

[24] Ruan Y, Li Z, Shen Y, Li T, Zhang H, Guo J. Functions of circular RNAs and their potential applications in gastric cancer. Expert Rev Gastroenterol Hepatol. 2020;14(2):85–92. https://doi.org/10.1080/17474124.2020.1715211.

[25] Buxbaum AR, Haimovich G, Singer RH. In the right place at the right time: visualizing and understanding mRNA localization. Nat Rev Mol Cell Biol. 2015;16(2):95–109. https://doi.org/10.1038/nrm3918.

[26] Komori T: Molecular Mechanism of Runx2-Dependent Bone Development. Mol Cells. 2020 Feb 29;43(2):168-175. doi: 10.14348/molcells.2019.0244.

[27] Zhao W, Yang H, Chai J, Xing L. RUNX2 as a promising therapeutic target for malignant tumors. Cancer Manag Res. 2021 Mar 16;13:2539-2548. doi: 10.2147/CMAR.S302173. eCollection 2021.

Figures and legends:

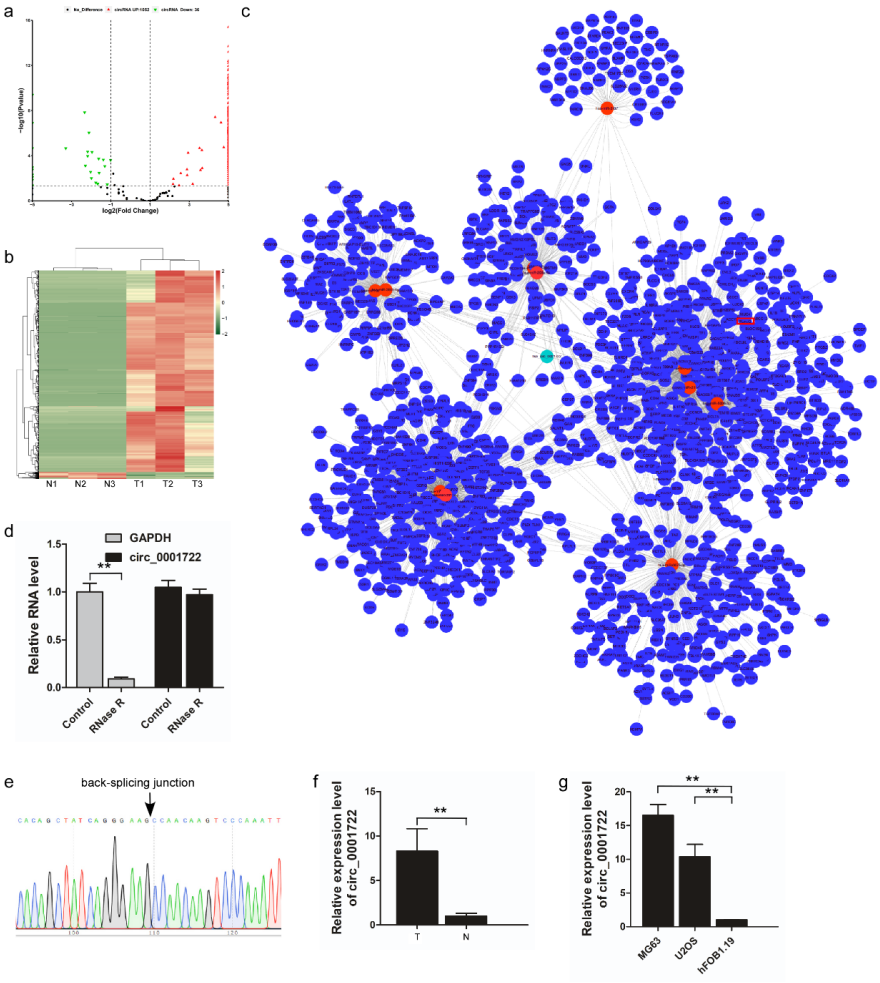

Figure 1. Identification and validation of differential expression of circ_0001722 in OS tissues and corresponding adjacent nontumor tissues. a: CircRNA expression profiling between two groups is showed with volcano plot. The vertical lines refer to a 2.0-fold (log2 scaled) up-regulation and down-regulation, respectively. The horizontal line corresponds to a P value of 0.05 (-log10 scaled). The red points represent up regulated circRNAs with statistical significance, and green points represent down regulated ones. b: Hierarchical clustering heatmap indicates differences in circRNA expression profiling between the two groups. c: 11 target miRNAs of circ_0001722 are predicted by miRanda and TargetScan, as well as their corresponding target cancer related mRNA, estimated by miRTarBase database. Green: circ-0001722; red: miRNAs; blue: mRNAs. d: Relative levels of circ_0001722 and GAPDH in OS cell line MG63 after their RNAs are treated with or without RNase R digestion. e: The validation of back-splicing junction sites of circ_0001722 by Sanger sequencing. f: The relative expression of circ_0001722 was detected in 20 OS tissues and corresponding adjacent nontumor tissues. (b) The relative expression of circ_0001722 was detected in two OS cell lines and an immortalized human fetal osteoblastic cell line.P <0.01.

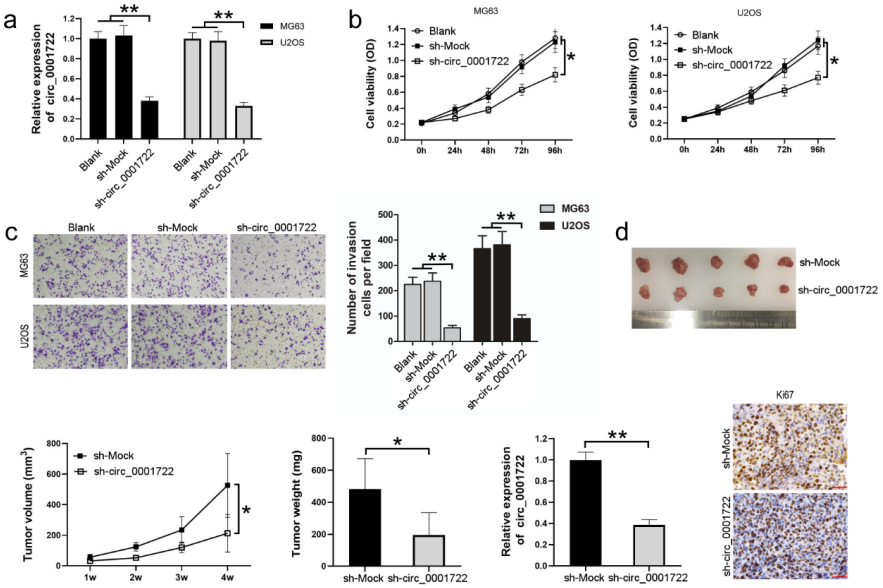

Figure 2. Downregulation of circ_0001722 suppresses cell proliferation of human OS cells. a: circ_0001722 is down-regulated by exogenous shRNA (sh-circ_0001722) in two human OS cell lines. b: Down-regulation of circ_0001722 can suppress cell proliferation of both human OS cell lines*in vitro* . c: Downregulation of circ_0001722 can suppress the invasion ability of both human OS cell lines. d: Downregulation of circ_0001722 can suppress cell proliferation of MG63 cells*in vivo* .P <0.05.P <0.01.

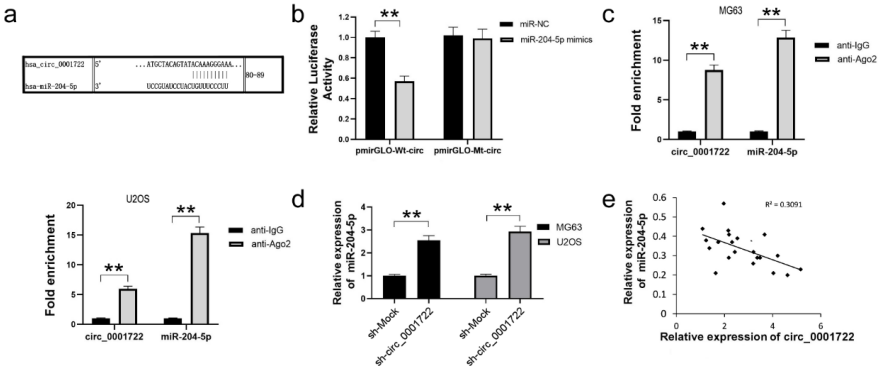

Figure 3. circ_0001722 binds to miR-204-5p to suppress its expression in human OS cells. a: Computational algorithms predicts complementary sequences of the circ_0001722 and miR-204-5p binding sequence. b: Compared with miR-NC, miR-204-5p mimic can significantly reduce the luciferase activity of pmirGLO-Wt-circ clone in HEK293T cells. However, neither miR-NC nor miR-204-5p mimic can affect the luciferase activity of pmirGLO-Mt-circ clone. c: Ago2 RIP assay shows that Ago2 can significantly enrich circ_0001722 and miR-204-5p. d: Downregulation of circ_0001722 can promote miR-204-5p expression in both human OS cell lines. e: The expression of miR-204-5p was negatively associated with circ_0001722 in human OS tissues. NC: negative control. Wt: wild type. Mt: mutant type. P <0.01.

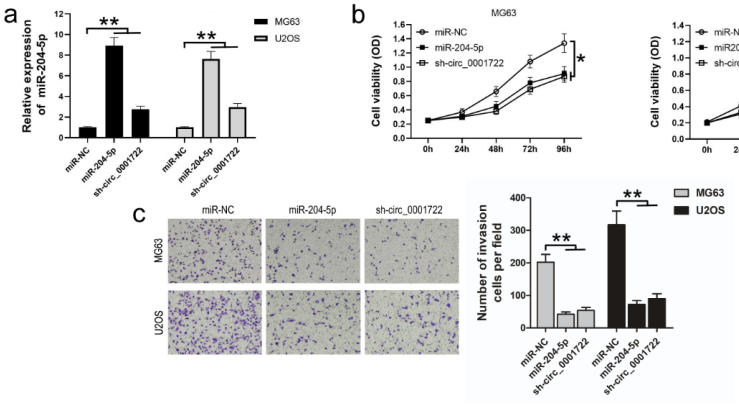

Figure 4. Sh-circ_0001722 suppresses proliferation and invasion of human OS cells by upregulating miR-204-5p. a: Both miR-204-5p and sh-circ_0001722 can upregulate miR-204-5p expression level in two human OS cell lines. b: Both miR-204-5p and sh-circ_0001722 can suppress cell proliferation of human OS cell lines *in vitro* . c: Both miR-204-5p and sh-circ_0001722 can suppress the invasion ability of human OS cell lines *in vitro* . NC: negative control. P <0.05.P <0.01.

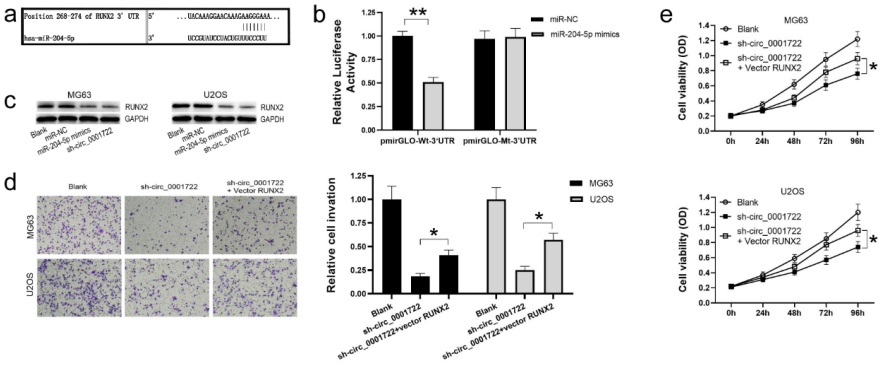

Figure 5. sh-circ_0001722 suppresses proliferation and invasion of human OS cells through miR-204-5p/RUNX2 axis. a: Computational algorithms predicts that miR-204-5p targets RUNX2 mRNA 3'UTR. b: Comparing with miR-NC, miR-204-5p can significantly reduce the luciferase activity of pmirGLO-Wt-3'UTR clone in HEK293T cells. However, neither miR-NC nor miR-204-5p can affect the luciferase activity of pmirGLO-Mt-3'UTR clone. c: Both miR-204-5p and sh-circ_0001722 can suppress RUNX2 expression in human OS cells. d: Suppression affect by downregulating circ_0001722 on cell proliferation can be rescued by exogenous RUNX2. e: Suppression affect by downregulating circ_0001722 on cell invasion can be rescued by exogenous RUNX2. NC: negative control. Wt: wild type. Mt: mutant type.P <0.05. P <0.01.

Supplementary files:

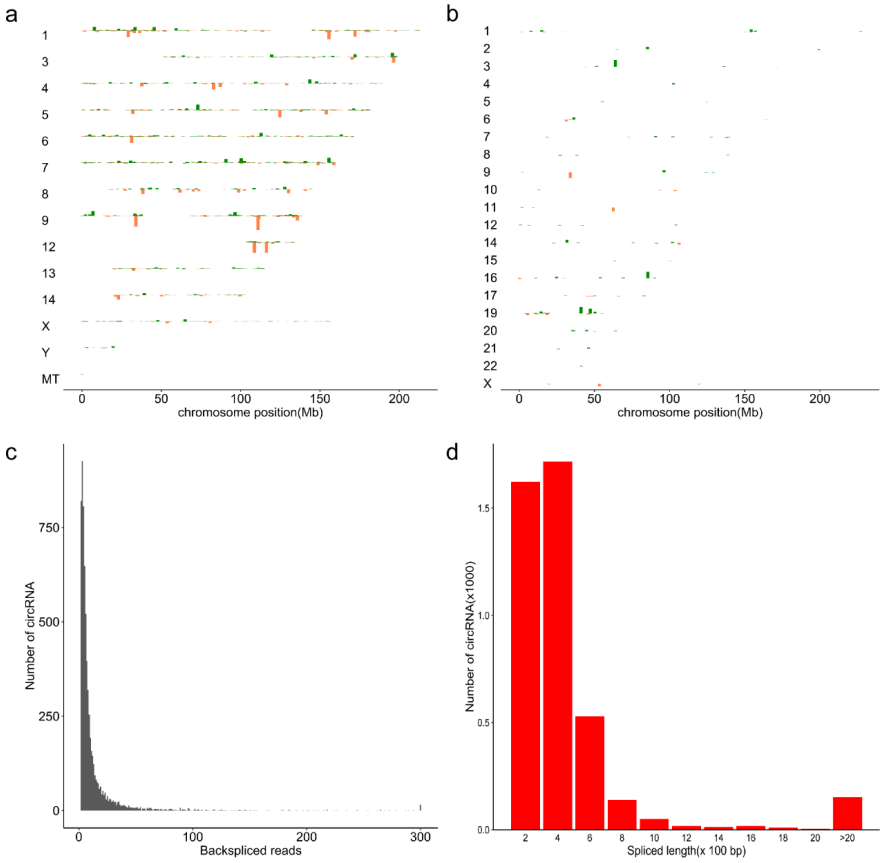

Supplementary Figure 1. Identification and annotation of circRNAs in OS and corresponding adjacent nontumor tissues. a and b: The chromosome distribution of total identified circRNAs in OS tissues (a) and corresponding adjacent nontumor tissues (b) samples, separately. Y-axis: chromosome number; X-axis: chromosome position; green: positive strands; orange: negative strands. c: Distribution of back-spliced reads after two rounds of filtering out false-positive candidate circRNAs. d: The length distribution of identified circRNAs.

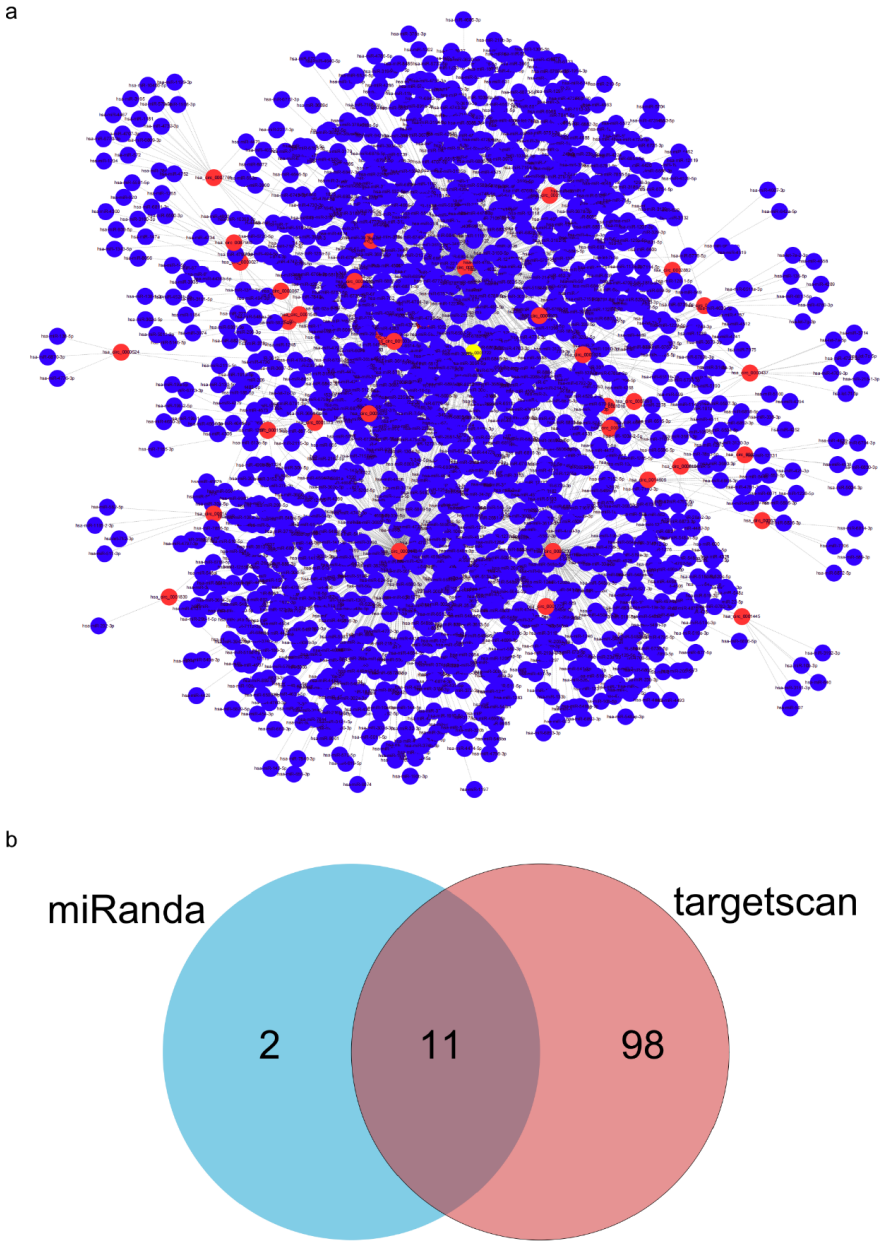

Supplementary Figure 2. The circRNAs-miRNAs interaction network. a: The circRNAs-miRNAs interaction network of predicted 36 differentially expressed circRNAs. Yellow: circ_0001722; red: circRNAs; blue: miRNAs. b: Regarding circ_0001722, there were 11 overlapped regulatory pairs between miRanda and TargetScan.

Supplementary Table 1. The clinicopathological characteristics of OS patients

Characteristic	**Case n (%)**
Gender	
Male	12(60)
Female	8(40)

Characteristic	**Case n (%)**
Age/year	
¡18	14(70)?¿?
18	6(30)
Clinical stage	
I	1 (5)
II	14(70)
III	5(25)
Tumor size	
¡8cm	5(25)?¿?
8cm	15(75)
Location	
Tibia	7(35)
Femur	11(55)
other	2(10)
Subtype	
Osteoblastic	8(40)
Chondroblastic	7(35)
Fibroblastic	3(15)
Mixed	2(10)

Supplementary Table 2. The primers used in this study

Name	Name	Sequence
circ_0001722	Forward	TAGCTCTGAAGGTGATCAGGC
	Reverse	CCTTCCCCTAGTTTTTCCAGC
miR-204-5p	Forward	ACACTCCAGCTGGGTTCCCTTTGTCATCCTAT
	Reverse	CTCAACTGGTGTCGTGGA
GAPDH	Forward	AACGTGTCAGTGGTGGACCTG
	Reverse	AGTGGGTGTCGCTGTTGAAGT
U6	Forward	GCTTCGGCAGCACATATACTAAAAT
	Reverse	CGCTTCACGAATTTGCGTGTCAT